Enhanced Estimation of the Rotor Position of MV-Synchronous Machines in the Low Speed Range

Simon Feuersänger, Mario Pacas
Universität Siegen, Germany
Simon.Feuersaenger@uni-siegen.de, jmpacas@ieee.org

***Abstract*—In the past, plenty of identification methods have been proposed for the encoderless control of induction machines and of permanent magnet synchronous machines, including all important tasks of the encoderless operation, such as the identification of the initial rotor position, the low and the high speed operation of the drive. However, not all the available methods are suitable for the application on electrically excited synchronous machines (EESM) with damper winding, which are commonly used in high power, medium voltage (MV) applications. For a large class of EESM the known methods of encoderless control fail in delivering the correct estimation of the rotor position especially in the low speed range of operation. In the present work the problems related to the encoderless control of the EESM with conventional techniques are described and a new approach is introduced, which injects low frequency test signals to identify the rotor position. In the same way the model based methods are enhanced and a persistent operation at low and zero speed becomes possible. Measurement results on a conventional medium voltage inverter validate the applicability of the proposed scheme.**

Keywords—Sensorless control; wound rotor synchronous machine, wound field synchronous machine, electrically excited synchronous machine

I. INTRODUCTION

The classical fields of operation for inverter fed electrically excited synchronous machines (EESM) are high power, medium voltage (MV) applications, generally with power ratings above several megawatts. In this power range, the EESM is often preferred to the induction machine (IM) due to constructive issues like a larger possible air gap or less rotor losses leading to a simpler cooling system. Permanent magnet synchronous machines (PMSM) are rarely used for high power ranges because of their expensive magnet materials. In the last years, the EESM also became attractive for electrical vehicles due to its good performance in the field weakening area, which is essential in those applications [1]. In this case, a moderate power, low voltage (LV) machine is required. A great difference regarding the machine design compared to the MV applications is the absence of the damper winding in most of the latter applications.

The control of an EESM or of any AC machine in general demands the information of the angular position of a certain space phasor that describes the machine. This information can be obtained by a machine model, which is fed by the measured machine currents and the rotor angle that is measured with an encoder. In this way, the control in any operating point in the whole speed range is possible. Nevertheless, the dependence on a mechanical sensor is undesirable either because of higher costs, not only caused by the sensor itself but also because of higher installation times, wiring accessibility etc., or especially because of the reduction of the total reliability when using the sensible sensor, as it is prone to failures. The control without mechanical angular sensor was an important topic of research in the last decades, mainly focusing on PMSMs or IMs in the low voltage range [2]-[3]. Until now, different encoderless approaches need to be combined in order to cover the whole speed range of an AC machine. Methods for the moderate or high speed range (typically above 3 to 5% of the nominal speed) base on the integration of the induced stator voltage can be applied without difficulties to any machine including EESMs [4]-[5]. However, control schemes for the low-speed range as well as approaches for identifying the initial rotor position need to inject additional, mostly high frequency, test signals (in this context "high frequency" means a much higher value than the machine nominal frequency). In that way, machine dependent asymmetries like rotor saliencies or saturation effects are identified to finally estimate the rotor position. Presently, plenty of such methods are available for PMSMs and IMs [6]-[7].

To answer the question if these well-known signal injection methods can also be applied to EESMs, it is necessary to distinguish between EESMs with or without a damper winding. In case of EESM without damper winding, many of the encoderless methods originally designed for PMSMs can also be applied with only minor changes e.g. compensation of the strong cross coupling effects in EESMs [8]. In fact, the encoderless control can even become easier as the machine exhibits one additional degree of freedom if compared with the permanent magnet type. In case of the EESM, not solely the stator winding but also the field winding can be used to either inject a test signal and analyze the reaction in the stator [8]-[14] or to analyze the response in the field winding caused by a current injection in the stator winding [15]. In those applications where a (low voltage) EESM with no damper winding is used [8], [12]-[14], usually a transistor converter with high switching frequency feeds the field winding. Thus, the frequency of the test signal can be very high, achieving a high dynamic identification of the rotor position.

However, the conditions for medium voltage EESM with damper winding are completely different. First, the damper winding influences strongly the high frequency admittance of the stator winding, making it hard or even impossible to detect any angular dependence of the stator admittance, even in

978-1-4673-7151-3/15/$31.00 ©2015 European Union

salient pole machines. Consequently, nearly all high frequency injection methods, which are based on the evaluation of the stator quantities, fail in most machines of this type [17]-[18]. Besides, usually a low voltage thyristor inverter feeds the field winding and is operated at the low net frequency. The current measurement of these devices is mostly not designed to detect high frequency signals as it is also sampled with a low frequency (often six times the net frequency, e.g. 300 or 360Hz). Hence, the high frequency injection as well as the detection in the field winding cannot be achieved.

A possible solution to detect the rotor position in EESMs with a damper winding could be the injection of a lower frequency test signal (much lower than 300Hz) in the field winding. The drawback of this approach is, that the high dynamic control of the main inverter would reject the test signal as a disturbance on the stator side and impeding the identification [4]. Additionally, the impact at the stator side is very weak when a test signal is injected in the field winding [19]. Thus, this solution seems to be unsuitable for these EESMs.

The remaining solution, the injection of a low frequency test signal in the stator winding with evaluation of its response in the field winding, is now in the focus of this paper. When analyzing identification methods based on the injection of test signals for medium voltage drives, theoretical considerations alone are not enough, so the tight hardware restrictions of a conventional MV-inverter must also be taken into account. In particular, the very low switching frequency of these inverters (e.g. 250Hz), which often also needs to be reduced in the low-speed or standstill region (e.g. less than 150Hz) is one of the main challenges when injecting additional test signals. In the following, the novel identification procedure for MV-EESMs is explained and its applicability on a conventional inverter is examined.

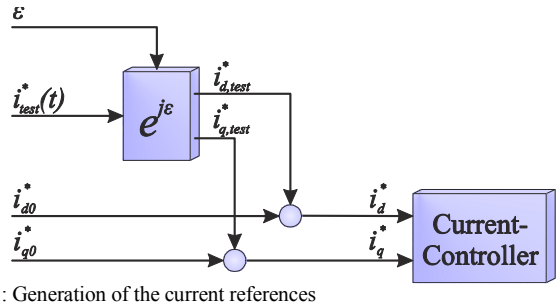

Fig. 1: Generation of the current references

II. Basic Idea

The basic idea of the presented method is that the injection of a signal in the d-axis of the machine on the stator side leads to a significant reaction in the field circuit whereas a test-signal in the q-axis has no influence on the field current. In this approach an alternating current test signal $i_{test}(t)$, injected with an angular orientation ε relative to the d-axis is proposed. As the rotor position needs to be identified during the normal operation of the drive, the test signal, or more precisely its reference $i^*_{test}(t)$, is added to the current reference values i^*_{d0} and i^*_{q0} that are delivered by the superimposed control (i.e. velocity control) to obtain the desired torque and magnetic flux. The resulting current references i^*_d and i^*_q are the inputs of a current controller, e.g. PI-controller, hysteresis control, etc. (Fig. 1).

If the test signal, i.e. a sine signal, is applied in the q-axis (ε=90°), the field winding does not show any measurable change as long as the rotor position is correctly identified or known (Fig. 2b). Yet, if there is an error γ_{Error} between the identified position γ_i of the identified d-axis d_i and the real rotor position γ, the test signal will produce a current component in the real d-axis (Fig. 2 a and c). Based on the

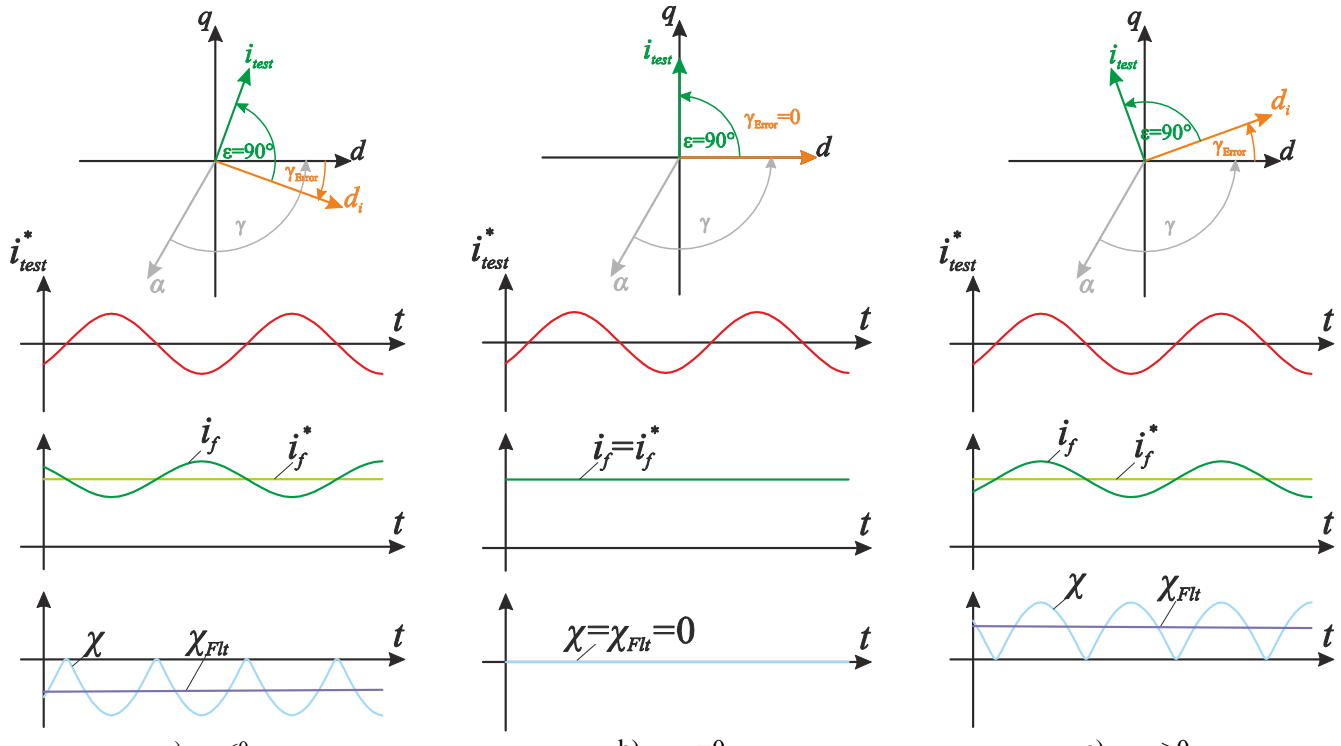

a) γ_{Error}<0 b) γ_{Error}=0 c) γ_{Error}>0

Fig. 2: Current response in the field winding for different angular errors in the estimation of the rotor position

measurable answer in the field current, the identified rotor position γ_i can be adapted or in other words, the error γ_{Error} of the estimation can be minimized.

Fig. 2 also depicts the principal answer of the field current i_f to an excitation in the identified q-axis for the three cases $\gamma_{Error}<0$, $\gamma_{Error}=0$ and $\gamma_{Error}>0$. As already stated if the d-axis is correctly identified, the field circuit is not influenced by the test signal (Fig. 2b) and follows the desired reference trajectory. If the identified rotor position is not correct, the field current is distorted and differs from its reference. An error γ_{Error} can occur due to inaccurate parameters of the model or to a drift or offsets in the voltage integration, on which the sensorless model is based.

Depending on the sign of the error γ_{Error}, the phase of the additional component of the field current that results from the injected test signal differs by 180° (compare Fig. 2 a and c) and can be analyzed for obtaining more information about the position error. It is important to point out that for gaining a measurable response in the field circuit, slow dynamics of the current control in the excitation system is required. Otherwise, the control of the field circuit will consider the current produced by the test signal to be a disturbance and would try to reject it. Fortunately, in practical MV-EESMs the current control of the exciter is rather slow.

For the automatic correction of the angular error it is convenient to define an "indicator" as a single variable that contains as much information as possible about the error that is considered. Thus a variable χ is introduced that fulfills this function and bundles the information contained in the field current in just one quantity and is defined by multiplying the error signal (i_f-i_f^*) with the per unit value of the test signal:

$$\chi(t) = \left(i_f - i_f^*\right) \cdot \frac{i_{test}^*(t)}{\hat{i}_{test}} \tag{1}$$

$$i_{test}^*(t) = \hat{i}_{test} \cdot \sin\left(2\pi f_{test} t\right) \tag{2}$$

with: $\chi(t)$ the proposed indicator, $\hat{i}_{test}$ the amplitude of the test signal and f_{test} the frequency of the test signal

The indicator $\chi(t)$ defined in this manner becomes zero if the error $\gamma_{Error}=0$. For negative errors $\gamma_{Error}<0$ the indicator function pulsates and exhibits a negative mean value, conversely for $\gamma_{Error}>0$ the mean value of $\chi(t)$ becomes positive (Fig. 2). For the proposed procedure the mean value of $\chi(t)$ builds the base for the correction of the error and therefore only the filtered value of $\chi(t)$ is utilized (χ_{Flt}) and it is acquired with the help of a continuous window integration over the last period of the signal.

III. Correction Mechanism

The indicator defined above allows the correction of an already estimated rotor position. As explained at the beginning the screening effect of the damper winding as well as the low

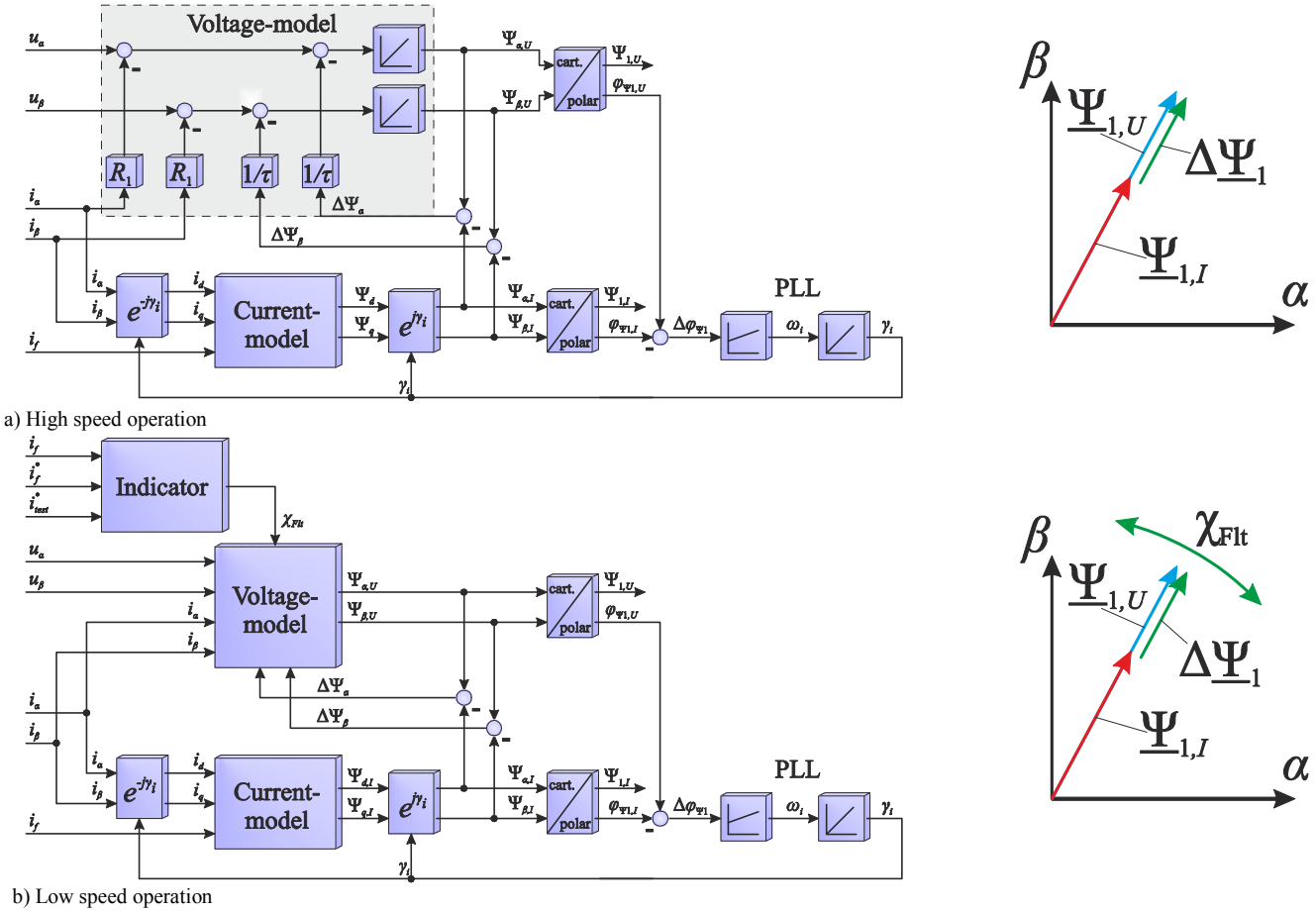

a) High speed operation

b) Low speed operation

Fig. 3: Adaption of the stator flux obtained by the voltage-model in encoderless operation at a) high-speed and b) low speed

sample time for the field current measurement demands a low frequency test signal (20… 100 Hz) with the evident drawback of a slow dynamic. Therefore, this method cannot be used alone for the encoderless control. Especially for dynamical changing loads, the procedure fails. However, if the proposed indicator is combined with a method that exhibits good dynamics in the high velocity range the advantages of each of the schemes compensate the drawbacks of the other.
Hence, the rotor position can be estimated with a standard scheme and in the region of low mechanical velocities it is continuously adjusted in an additional adaptation loop by using the proposed indicator.

Fig. 3b shows the structure of such a combination of a Model Reference Adaptive System (MRAS) together with the proposed correction. To understand the proposed scheme, first the operation at high speeds, without angular correction by the indicator is explained (Fig. 3a) [4]. In this scheme, two machine models are calculated simultaneously: the voltage model, which serves as the reference model and the current model which is adapted. The current model requires the (identified) rotor position γ_i as input, which is obtained by a phase locked loop (PLL). This PLL adjusts the identified rotor position γ_i in such a way that the stator flux space phasor that is calculated by using the current model $\underline{\Psi}_{I,I}$ is aligned with the reference stator flux $\underline{\Psi}_{I,U}$ that is calculated by the voltage model. Thus, the rotor position is correctly identified. However, the voltage model needs to be damped in order to overcome the well-known drift problem of the open voltage integration in the low frequency range. In the present proposal the current model suppresses the offset drift inherent to the voltage model by slowly adjusting the absolute value of stator flux computed by the voltage model to the one obtained by the current model (Fig. 3a right). The time constant τ of this correction can be chosen very large, as only the weak drift of the voltage model needs to be compensated. This mechanism has a corrective effect on the amplitude of the space phasor of the stator flux $\Psi_{I,U}$ but not on its phase $\varphi_{\Psi I,U}$. Therefore, in the low velocity range and especially in stand still the correction of the phase is mandatory.

This is indeed the main contribution of the present proposal: to achieve the adjustment of the phase $\varphi_{\Psi I,U}$ of the flux space phasor by applying the idea explained above. As described in the last section the filtered indicator χ_{Flt} provides the information about the error of the rotor position γ_{Error} and can be used for its correction. However, the correction of the identified rotor position γ_i has to consider that the γ_i value is also adjusted by the PLL as shown in Fig. 3a. Thus the PLL would act against the correction and set the phase to the old value within few sample times. Yet a further analysis of the structure of Fig. 3a indicates that in case of a perfect current model with correct values of the parameters an estimation error γ_{Error} can only occur, when the voltage model computes an erroneous value of the stator flux space phasor $\underline{\Psi}_{I,U}$. Hence, the proposed indicator χ_{Flt} will be used for reducing primary the angular error of the voltage model as shown in Fig. 3b and as a consequence the error in the identified rotor position will also be reduced.

This correction is achieved by continuously rotating the stator flux space phasor $\underline{\Psi}_{I,U}$ with the correcting angular velocity ω_{corr}, directly derived from the measured indicator value χ_{Flt} as:

$$\omega_{corr} = -2\pi \cdot \frac{\chi_{Flt}}{\chi_{Flt,max}} \cdot k_{corr} \tag{3}$$

Thus, the indicator χ_{Flt} is first normalized to its maximum value $\chi_{Flt,max}$ in order to ensure same dynamic behavior of the correction mechanism for different machines. Being $\chi_{Flt,max}$ the indicator value when purposely injecting the test signal in the d-axis (ε=0°). This value can be measured once during the commissioning of the drive. The resulting constant k_{corr} determines the dynamic of the correction. As an example, the standard value k_{corr}=1.0 1/s rotates the stator flux with one revolution per second when the maximum indicator (at an angular error of γ_{Error}=90°) is present.

The correction is performed with the same sample time T_S used for the calculation of the voltage model. During a sample "k", first the voltage integration as shown in the block diagram in Fig. 3a is performed (eq. 4) and the resulting stator flux space phasor is stored in the variable $\underline{\Psi}'_{1,U}(k+1)$. Then, this value of the stator flux space phasor is rotated in a second step by the angular value "$\omega_{corr} \cdot T_S$" to achieve the correction of the phase of the stator flux, based on the indicator value (Eq. 6 and Fig. 4) according to the following equations:

$$\Psi'_{1,U}(k+1) = \Psi_{1,U}(k) + \left(\underline{u}_1 - R_1 \underline{i}_1 - \frac{\Delta\underline{\Psi}_1(k)}{\tau} \right) \cdot T_S \tag{4}$$

$$\Delta\underline{\Psi}_1(k) = \Psi_{1,U}(k) - \Psi_{1,I}(k) \tag{5}$$

$$\Psi_{1,U}(k+1) = \Psi'_{1,U}(k+1) \cdot e^{j\omega_{corr} T_S} \tag{6}$$

with:

- $\underline{u}_1$: Stator voltage space phasor
- $\underline{i}_1$: Stator current space phasor
- R_1: Stator resistance
- τ: Time constant of the correction by the current model

In that way the value of the stator flux space phasor for the next sample "k+1" is obtained.

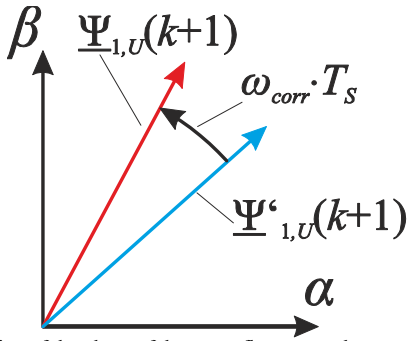

Fig. 4: Correction of the phase of the stator flux space phasor

If the rotor position is identified correctly, the indicator χ_{Flt} and finally ω_{corr} ideally become zero and thus no rotational correction is performed. In this case, only the corrective effect of the current model is active which eliminates the offset drift in the absolute value of the stator flux obtained by the voltage model. However, if an angular error is identified by the indicator χ_{Flt}, the phase of the identified stator flux space phasor is adjusted as well, until the error becomes finally zero.

IV. Measurement Results

To validate the new encoderless approach, measurements were carried out on a test bench for medium voltage drives containing a conventional medium voltage inverter which feds a direct excited synchronous machine with damper winding. Unfortunately, the coupled load machine (induction machine) exhibits a lower nominal torque so that the synchronous machine could not be loaded with more than ¼ of its nominal torque. The inverter and machine data are given in Table 1 to 3. Fig. 5 shows a photo of the test bench.

Table 1: Inverter Data

Name	ACS 6000		
Topology	3-Level NPC inverter with IGCTs	S_N	3MVA
I-measurement	10Bit, Range: ±1228A	U_{dc}	4670V

Table 2: Synchronous Machine Data

P_N	1.0MW	n_N	225min^{-1}	f_N	15Hz
U_N	3300V	I_N	186A	$cos\ \varphi_N$	1.0

Table 3: Load Machine Data (Induction Machine)

P_N	870kW	n_N	712min^{-1}	f_N	60Hz
U_N	3300V	I_N	200A	$cos\ \varphi_N$	0.8

For practical reasons the developed adaptation procedure was applied to a stator current control scheme according to the proposal of [4]. This scheme is known as DMCC (**D**FLC **M**odulator Based **C**urrent **C**ontrol with DFLC as abbreviation for "**D**irect **F**lux **L**inkage **C**ontrol"), it has a high similarity to DTC (**D**irect **T**orque **C**ontrol). In principle, DMCC is a hysteresis control of the machine stator current, which sets the actual inverter switching state according to the state of the hysteresis control. Like all hysteresis controllers it leads to a variable switching frequency, in which the average value of the switching frequency is adjusted by the hysteresis bands. For the present research, this current controller was used because it could be easily implemented in the existing DTC-based drive without the need of changing the modulator. However, the principle idea of the encoderless proposal can also be applied to a field oriented control scheme or to any other current controller.

The first task to be accomplished is the proper choice of the test signal. Fig. 6 depicts the resulting reference values for the components of the stator current space phasor in dq-coordinates with the added test signals as well as the corresponding values of the actual current components. The test signal has a frequency of 20Hz and the hysteresis control is tuned so that an average switching frequency of 150Hz arises. As it can be appreciated in the measurement results, the

Fig. 5: Test bench for medium voltage drives

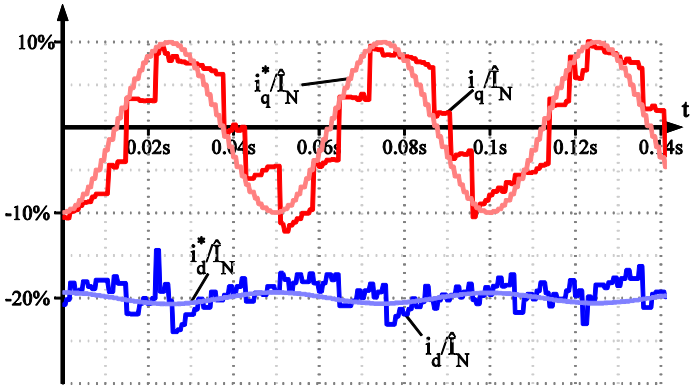

Fig. 6: Test signal quality, f_{test}=20Hz, avg. switching frequency: 150Hz

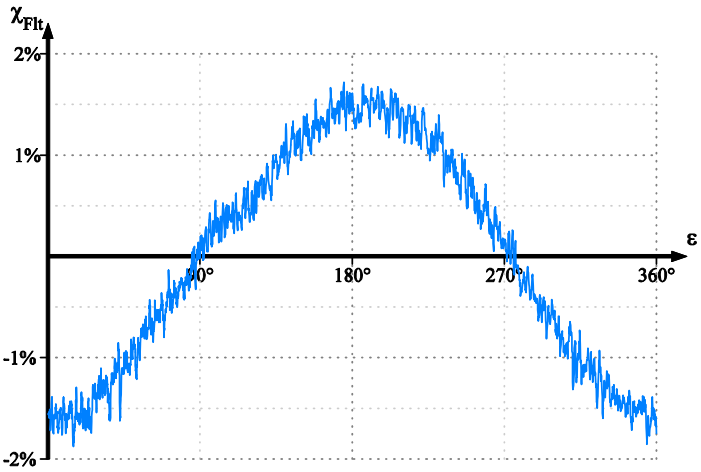

Fig. 7: Measured indicator for injecting the test signals in different angular positions ε

actual value of i_d and i_q can in principle follow the reference but there are significant discrepancies between the desired and the actual trajectories. The frequency of the test signal can certainly be increased but the width of the hysteresis control has to be correspondingly adapted to limit the average switching frequency. The resulting signals are thus of lower quality and the identification results that can be achieved with a test signal of higher frequency are not satisfactory. Conversely, the frequency of the test signal can be decreased and the quality of the signal and of the identification results become much better. However, this selection has a detrimental effect on the dynamic of the encoderless control. The utilized frequency of 20 Hz represents a compromise between signal quality and dynamics of the identification procedure. As a matter of fact, a high frequency of the test signal accompanied by high switching frequency is preferable, but it has to be taken into account that a MV-Inverter has the constrain of a limited switching frequency.

The choice of the test signal amplitude is a tradeoff as well. Of course, a higher amplitude of the test signal leads to a more pronounced reaction in the field circuit, easing the identification procedure. However, as the test signal is injected in the q-axis of the machine, it also generates an undesired torque component. For higher test signal amplitudes the torque and finally the shaft oscillation will increase, leading to a rough operation of the drive. Under no load condition, a test signal amplitude of 10% of the nominal machine current also leads to a ripple of 10% of the nominal torque. If the load is increased the torque ripple is lightly reduced (assuming a classical control of the machine with *cos* φ=1). On the other hand, decreasing the amplitude will not only reduce the reaction in the field winding but the test signal quality is reduced as well. This is because the inverter cannot follow fine changes in the current reference signal while working at a low switching frequency. Our experience in the lab points out that a test signal amplitude of 10% of the nominal machine current leads to the best tradeoff between signal quality, response in the field current and unwanted oscillation of the shaft.

In a second step the sensitivity of the indicator i.e. how pronounced is the influence of the injected stator current on the field circuit has to be examined. For this purpose, the machine was run under DMCC control and the 20Hz test signal with a phase angle ε with respect to the real d-axis of the machine was added to the references of the stator currents (Fig. 1) and impressed by the control. An encoder was used for the measurement of the actual rotor position and the phase ε of the impressed current space phasor was slowly increased (360° in 20s). The resulting filtered indicator χ_{Flt} can be plotted as a function of the phase angle ε as depicted in Fig. 7. This measurement shows that despite of the low quality of the resulting test current in the stator winding, the obtained indicator χ_{Flt} is suitable for being used in the correction method aimed in this work.

The real advantage of the adaption procedure presented in this work is the enhancement of the model based sensorless control schemes in the low velocity range. Usually speed reversal is possible by using a voltage model based control, providing that the riding through zero is fast enough and the voltage integration does not drift. Although the correction with the indicator χ can be applied in such cases, it does not result into a significant improvement. Different is a slow reversal or

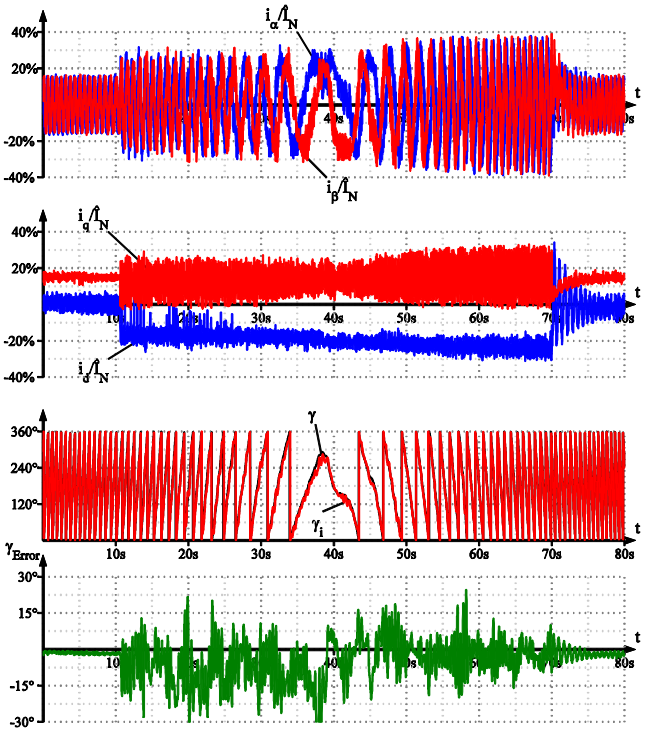

Fig. 7: Speed reversal from +40min^{-1} to -40min^{-1} in 80 seconds. M/M_N=25%

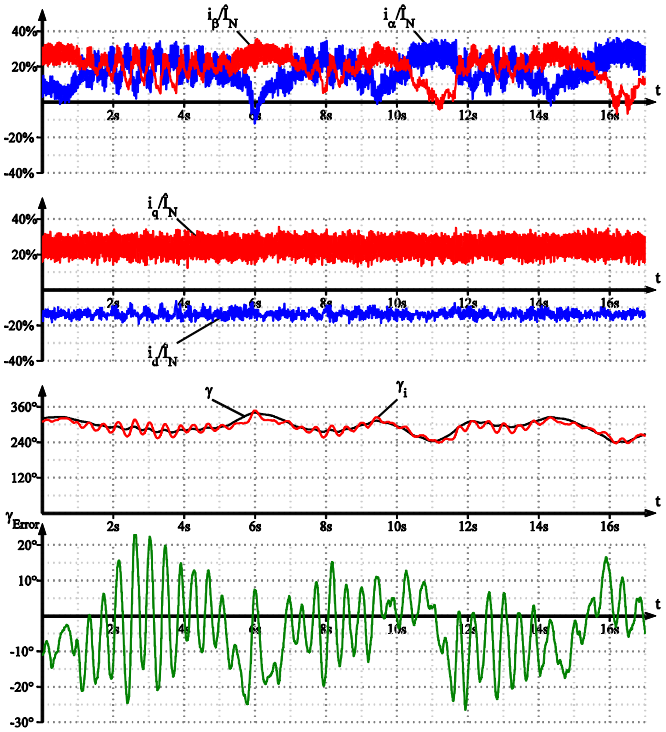

Fig. 8: Operation at standstill M/M_N=25%

the persistent operation at low velocity. If such speed profiles are required, the sensorless schemes based on the voltage model fail but if complemented by the correction proposed here they can work under low speed profiles. Fig 7 illustrates a speed reversal from +40min^{-1} to -40min^{-1} in 80 seconds. The torque on the machine under test was controlled to a constant value and the velocity profile was realized with the load machine in the same test bench. Fig. 8 shows the performance under same conditions but at standstill (small variations in the rotor angle are caused by the non-ideal velocity control of the load machine).

The measurement results demonstrate that the synchronous machine can be operated without encoder in the low speed range for unlimited time. The identified rotor position γ_i does not drift away and can be kept stable. The angular error γ_{Error} is depicted for the assessment of the quality of the identification procedure. The error exhibits a high ripple with a maximum value of 30°. Although the mean values of the stator current components follow their references they and as a result the torque present strong undesired oscillations.

The moderate quality of the identification procedure for the enhancement of the sensorless control can be attributed to the low frequency of the test signal that yields a slow dynamic behavior. Of course, an increase of the frequency of the test function alleviates this problem but is not always allowed. Especially in high power MV drives the maximum switching frequency has to be limited due to thermal constrains. As mentioned above, raising the frequency of the test signal without the corresponding increase of the switching frequency makes things even worse.

V. Conclusion

A novel encoderless control scheme for medium voltage electrically excited synchronous machines suitable for the low speed range was introduced. The approach is based on the injection of a low frequency test signal in the stator winding and the evaluation of the response in the field circuit for the correction of a combined voltage-current-model based control. Measurement results on a conventional medium voltage drive validate that the machine can be operated in the low speed range or at standstill for unlimited time. Due to constrains in the switching frequency of the inverter, the frequency of the test signal has to be kept at a rather low value of 20Hz. With this test signal frequency the dynamic of the angular correction is quite low and leads to a moderate performance regarding the accuracy of the identified angle. However, a stable operation can be guaranteed, as the identified angle does not drift.

References

[1] C. Rossi, D. Casadei, A. Pilati, and M. Marano, "Wound Rotor Salient Pole Synchronous Machine Drive for Electric Traction", Industry Applications Conference, 2006. 41st IAS Annual Meeting. Conference. Record of the 2006 IEEE , vol.3, pp.1235-1241, 8-12 Oct. 2006

[2] Pacas, M.; "Sensorless Drives in Industrial Applications", Industrial Electronics Magazine, IEEE vol. 5, no. 2, pp.16-23, June 2011

[3] Holtz, J.; "State of the art of controlled AC drives without speed sensor", Power Electronics and Drive Systems, 1995., Proceedings of 1995 International Conference on, pp.1,6 vol.1, 21-24 Feb 1995

[4] Niemelä, M., "Position Sensorless Electrically Excited Synchronous Motor Drive for Industrial Use Based on Direct Flux Linkage and Torque Control", Dissertation, Lappeenranta University of Technology, Lappeenranta, Finnland, 1999

[5] Boldea, I.; Andreescu, G.D.; Rossi, C.; Pilati, A.; Casadei, D., "Active flux based motion-sensorless vector control of DC-excited synchronous machines", Energy Conversion Congress and Exposition, 2009. ECCE 2009. IEEE, pp.2496,2503, 20-24 Sept. 2009

[6] Linke, M.; Kennel, R.; Holtz, J.; "Sensorless speed and position control of synchronous machines using alternating carrier injection", Electric Machines and Drives Conference, 2003. IEMDC'03. IEEE International, vol.2, pp.1211,1217 vol.2, 1-4 June 2003

[7] Holtz, J., "Sensorless Control of Induction Machines—With or Without Signal Injection?", Industrial Electronics, IEEE Transactions on, vol.53, no.1, pp.7,30, Feb. 2006

[8] Jongwon Choi; Ilsu Jeong; Kwanghee Nam; SungYoon Jung; "Sensorless control for electrically energized synchronous motor based on signal injection to field winding", Industrial Electronics Society, IECON 2013 - 39th Annual Conference of the IEEE, pp.3120,3129, 10-13 Nov. 2013

[9] Alaküla, M., "On the Control of Saturated Synchronous Machines", Dissertation, Dept. IEA, Lund Institute of Technology, Lund, Schweden, 1993

[10] Uzel, D.; Peroutka, Z., "Resolver Motivated Sensorless Rotor Position Estimation of Wound Rotor Synchronous Motors", Industrial Electronics (ISIE), 2013 IEEE International Symposium on, pp.1,6, 28-31 May 2013

[11] Uzel, D.; Smidl, V.; Peroutka, Z., "Estimator comparison for resolver motivated sensorless rotor position estimation of wound rotor synchronous motors", Power Electronics and Applications (EPE'14-ECCE Europe), 2014 16th European Conference on, pp.1,8, 26-28 Aug. 2014

[12] Rambetius, A.; Piepenbreier, B., "Sensorless control of wound rotor synchronous machines using the switching of the rotor chopper as a carrier signal", Sensorless Control for Electrical Drives and Predictive Control of Electrical Drives and Power Electronics (SLED/PRECEDE), 2013 IEEE International Symposium on, pp.1,8, 17-19 Oct. 2013

[13] Rambetius, A.; Piepenbreier, B., "Comparison of carrier signal based approaches for sensorless wound rotor synchronous machines", Power Electronics, Electrical Drives, Automation and Motion (SPEEDAM), 2014 International Symposium on, pp.1152,1159, 18-20 June 2014

[14] Xianming Deng; Lei Wang; Jiamin Zhang; Zhixun Ma, "Rotor Position Detection of Synchronous Motor Based on High-frequency Signal Injection into the Rotor", Measuring Technology and Mechatronics Automation (ICMTMA), 2011 Third International Conference on, vol.3, pp.195,198, 6-7 Jan. 2011

[15] Rambetius, A.; Ebersberger, S.; Seilmeier, M.; Piepenbreier, B., "Carrier signal based sensorless control of electrically excited synchronous machines at standstill and low speed using the rotor winding as a receiver", Power Electronics and Applications (EPE), 2013 15th European Conference on, pp.1,10, 2-6 Sept. 2013

[16] Feuersänger, S.; Pacas, M., "Initial Rotor Position Detection in Electrically Excited Medium Voltage Synchronous Machines", PCIM 2012, Nürnberg

[17] Feuersänger, S.; Pacas, M., "Initial rotor position identification in medium voltage synchronous machines", IECON 2012 - 38th Annual Conference on, pp.1852,1857, Oct. 2012

[18] Feuersänger, S.; Pacas, M., "Initial rotor position detection in synchronous machines using low frequency pulses", Industrial Electronics Society, IECON 2014 - 40th Annual Conference of the IEEE, pp.675,681, 29.10. – 01.11.2014